A DISCONTINUOUS GALERKIN METHOD FOR SIMULATIONS OF TRANSPORT PROCESSES ON THE PORE SCALE

CHRISTIAN ENGWER[1]

[1]Interdisziplinäres Zentrum für Wissenschaftliches Rechnen,
Universität Heidelberg, Im Neuenheimer Feld 368, 69120 Heidelberg

Abstract

In the simulation of pore scale processes a good approximation to the geometrical shape of the solid phase is crucial to good quality of the numerical results, while on the other hand interest often focuses on a small number of unknowns.

I will present a new approach for solving PDEs in complex domains. It is based on a Discontinuous Galerkin (DG) discretization on a structured grid, where the minimal number of unknowns is independent of the shape of the domain, while this new method still allows the provision of fine structures of the domains shape, even if their size is significantly smaller than the grid cell size. Its advantage for flow and transport simulation on the pore scale is that the resolution of the simulation can be chosen freely between very large domains, perhaps the size of several REVs, and very small domains, just the size of few sandcorns, without changing the discretization and without neglecting details in the shape of your domain.

1. INTRODUCTION

Classical numerical methods require a grid resolving the complicated geometry. Creating such grids is a highly involved process especially if coarse grids and high quality are required. Several methods have been developed that circumvent this problem. They are based on the use of a structured background mesh that encloses the domain. The Fictitious Domain method [GPP71, BDGG71] discretizes the PDE on the background mesh and adds the boundary conditions as additional constraints. This leads in general to a saddle point formulation that might be difficult to solve. The Composite Finite Element method [HS91] constructs piecewise linear basis functions on the fine background mesh und truncates them at the true boundary. Coarse grid basis functions for a geometric multigrid solver are constructed as combinations of fine grid basis functions. This method has been designed with emphasis on the fast solution of the arising linear system.

Our new method is based on the observation that in discontinuous Galerkin finite element methods the form of the element can be quite arbitrary. Thus the elements can be taken as the intersection of the structured background mesh with the complicated geometry. Assembling the stiffness matrix then requires integration over the interior and boundary of those non-standard elements. This is accomplished by constructing a local

triangulation within each element. Note that the local triangulations of different elements are completely independent.

In the following we will give an abstract description of the goals. Next we introduce into the new approach, especially considering the cases not coverd by standard error estimations and then we will numerically study these problematic cases for an elliptic model problem.

2. PROMBLEM DESCRIPTION

Let $\Omega \subseteq \mathbb{R}^d$ be a domain and $\mathcal{G}$ a partition of Ω into subdomains

$$\mathcal{G}(\Omega) = \left\{\Omega^{(0)}, \ldots, \Omega^{(N-1)}\right\}. \tag{1}$$

The partition $\mathcal{G}$ is usually based on some geometrical properties retrieved from experiments or previous simulations. The boundaries $\partial\Omega^{(i)}$ may have a complicated shape. The partition $\mathcal{G}$ and with it $\partial\Omega^{(i)}$ may change in time.

On each $\Omega^{(i)}$ we want to solve a partial differential equation

$$L_i(u_i) = f_i \tag{2}$$

with a differential operator L_i together with suitable boundary conditions on $\partial\Omega$ and transmission conditions on the interfaces $\Gamma^{(i,j)}$.

3. DISCONTINUOUS GALERKIN APPROACH

In our approach a triangulation $\mathcal{T}$ of Ω is given in addition to the domain Ω and the partition $\mathcal{G}$.

$\mathcal{T}$ is a structured partition of Ω, where the mesh size

$$h = \min\left\{\operatorname{diam}(t), |t \in \mathcal{T}\right\} \tag{3}$$

is not determined by the shape of Γ. $\mathcal{T}$ is chosen in such a way that the differential equations L_i can be solved with a desired accuracy.

The elements of the mesh are denoted by

$$\mathcal{T}(\Omega) = \left\{E_0, \ldots, E_{M-1}\right\}. \tag{4}$$

For all E_k there exists a bijective mapping T_{E_k} to a reference element $\hat{\Omega}$

$$E_k = T_{E_k} \circ \hat{\Omega}. \tag{5}$$

For each $\Omega^{(i)} \in \mathcal{G}$ (see Figure 1) we can define a triangulation

$$\mathcal{T}(\Omega^{(i)}) = \left\{E_n^{(i)} \,\middle|\, E_n^{(i)} = \Omega^{(i)} \cap E_n \vee E_n^{(i)} \neq \emptyset\right\} \tag{6}$$

Note that $E_n^{(i)}$ is always a subset of E_n, therefore we will call E_n fundamental element of $E_n^{(i)}$. There are no restrictions on the shape of $E_n^{(i)}$.

Conforming trial functions depend on the shape of the elements. This makes it very difficult to use them in our context as one does not have a predefined set of reference elements for which to supply a set of shape functions. Each $E_n^{(i)}$ can be shaped arbitrarily. Therefore we use a Discontinuous Galerkin scheme (DG) with a discontinuous piecewise polynomial approximation.

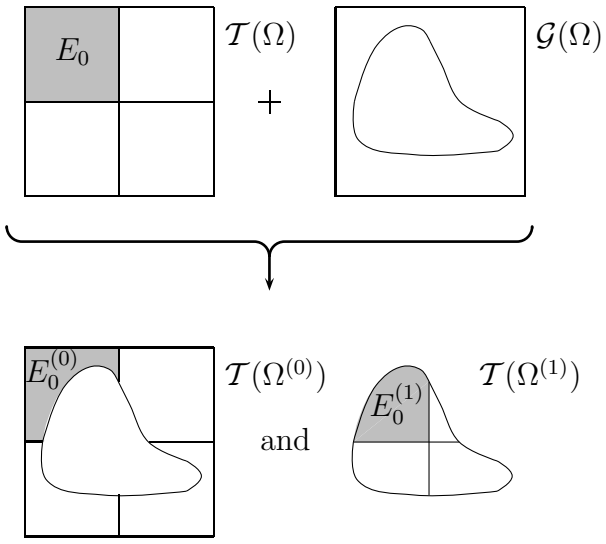

FIGURE 1. Construction of the partitions $\mathcal{T}(\Omega^{(i)})$ from the partitions $\mathcal{G}$ and $\mathcal{T}$ of the domain Ω.

On each element $E_n^{(i)}$ we choose a local polynomial base function set $\{\varphi_{n,j}^{(i)}\}$ with

$$\text{supp}(\varphi_{n,j}^{(i)}) = \bar{E}_n^{(i)} \tag{7}$$

Using DG, our trial functions can be chosen independently from the shape of the element. In [DFS03] it is shown that star shaped elements are sufficient, although not necessary, for the convergence rate to be independent of the shape of the elements. Furthermore certain DG formulations are element wise mass conservative and therefore able to accurately describe fluxes over element boundaries. A similar approach is also used in structural mechanics ([HH04]).

We choose our local base functions $\varphi_{n,j}^{(i)}$ as polynomial functions $\varphi_{n,j}$ defined on the fundamental element E_n and restrict their support to $E_n^{(i)}$:

$$\varphi_{n,j}^{(i)} = \begin{cases} \varphi_{n,j} & \text{inside of } \bar{E}_n^{(i)} \\ 0 & \text{outside of } E_n^{(i)} \end{cases} . \tag{8}$$

Assembling the stiffness matrix in DG only requires evlation of integrals over the volume of elements $E_n^{(i)}$ and the surface $\partial E_n^{(i)}$. Therefore we subdivide $E_n^{(i)}$ into easily integrable smaller objects. This means that we create a disjoint set $\{E_{n,k}^{(i)}\}$ of simple geometric objects, i.e. simplices and hypercubes.

Following equation (5) we define $E_{n,k}^{(i)}$ by a reference element $\hat{\Omega}$ and a transformation $T_{E_{n,k}^{(i)}}$ as

$$E_{n,k}^{(i)} = T_{E_{n,k}^{(i)}} \circ \hat{\Omega}. \tag{9}$$

To reduce the number of generated integration parts $E_{n,k}^{(i)}$ and still keep a high accuracy we allow curved boundaries for '$E_{n,k}^{(i)}$, which are represented by second order polynomials.

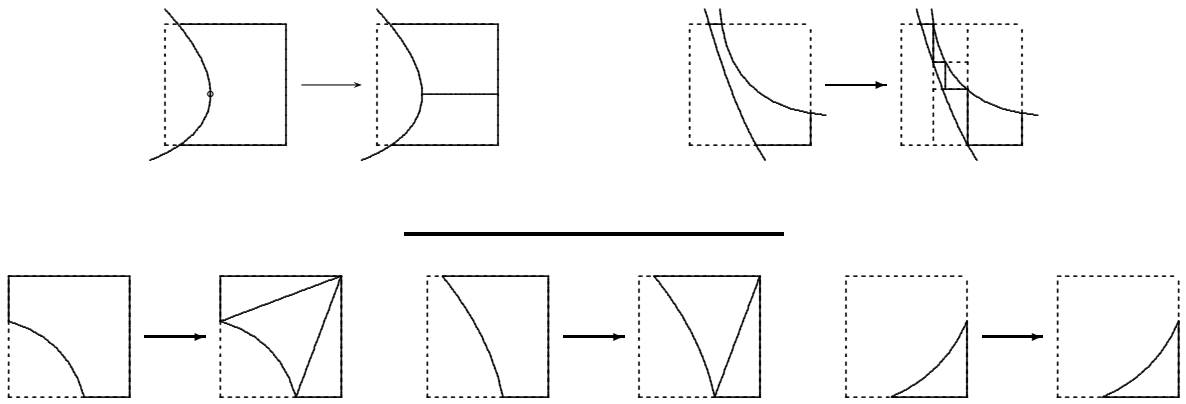

FIGURE 2. In the case of $\Omega \subset \mathbb{R}^2$, using suitable bisection strategies (upper figures), we have to destinguishe only three different cases (lower figures).

3.1. **Local triangulation.** In the following we will describe the conceptual of the local triangulation algorithm and illustrate these refering to Ω as $\Omega \subset \mathbb{R}^2$.

Our local triangulation consists of two parts. We first use a bisection on E_n to create a set $\{R_{n,k}\}$ of sub-rectangles. We now assign each $R_{n,k}$ to an class according to the way $R_{n,k}$ intersects with the interfaces $\Gamma^{(i,j)}$. Choosing suitable rules to control the bisection we obtain a small set of classes. For each of these classes we predefine a suitable triangulation.

Since the we assume that the geometry of the non-standard element is not too complicated, we found that for the case of $\Omega \subset \mathbb{R}^2$ two bisection rules and three triangulation cases are sufficient (Figure 2). For further details of the triangulation algorithm we refer to [EB05].

In the case of $\Omega \subset \mathbb{R}^2$, the recursive bisection is controlled by two rules.

4. NUMERICAL STABILITY

4.1. **Interpolation error.** Given are a function u and an interpolation Operator I mapping to the space of piecewise continuous polynomials. The interpolated function is denoted as

$$u^I = I \circ u \tag{10}$$

To get an estimation of the interpolation error one usually uses the Bramble-Hilbert lemma [BH70]. Using the Bramble-Hilbert lemma it is possible to give estimations of the error measured in the L_2-norm and the H^1-norm. In the optimal case it is

$$||u - u^I||_{L_2} \propto \quad O(h^{p+1}) \tag{11}$$

$$||u - u^I||_{H^1} \propto \quad O(h^p). \tag{12}$$

A prerequisite for these estimations is that the domain satisfies a strong cone property. In our case the elements $E_n^{(i)}$ might not fulfill this cone property. Elements with a cusp in one corver pose particular problems. As the tangential vectors of both edges are parallel in the corner the cone condition is violated (see Figure 3). Furthermore the element becomes anisotropic when refining the grid. To our knowledge there exist no estimations of the interpolation error of the solution on such cusp elements.

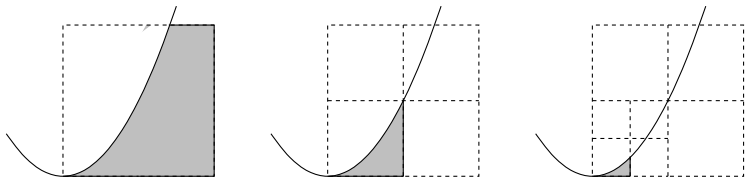

FIGURE 3. Refinement of cusp elements results in anisotropic elements, which do not fulfill the cone property.

We studied the interpolation error measured in L_2- and H^1-norms for a single element. To avoid numerical inaccuracies we did these calculations with MAPLE. When using Lagrange interpolation we observed optimal convergence for both the error in L_2- and in H^1-norm. When using L_2 projection we have no control over the derivatives and so we loose one order in the error convergence in the H^1-norm (see Figure 4).

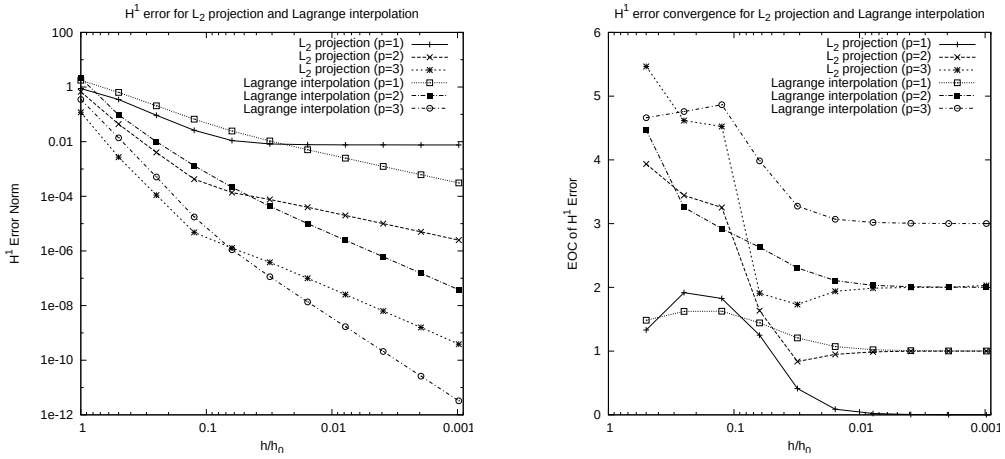

FIGURE 4. H^1 error and its convergence for L_2 projection and Lagrange interpolation on cusp elements.

4.2. **Elliptic model problem.** We now investigated the case of cusp elements, considering the following elliptic model problem in d space dimensions

$$\nabla \cdot j = f \ \text{ in } \Omega \subseteq \mathbb{R}^d \qquad j = -K\nabla p, \tag{13}$$

subject to boundary conditions

$$p = g \ \text{ on } \Gamma_D \subseteq \partial\Omega, \qquad j \cdot n = J \ \text{ on } \Gamma_N = \partial\Omega \setminus \Gamma_D. \tag{14}$$

We approximate the pressure p in the space of discontinuous finite element functions of order k

$$V_k = \{v \in L_2(\Omega) \mid v|_E \in P_k, E \in \mathcal{T}(\Omega)\} \tag{15}$$

where $\mathcal{T}(\Omega) = \{E_1, \ldots, E_n\}$ is a partition of Ω into non-overlapping elements and P_k is the set of polynomials of at most degree k. By Γ_{int} we denote the set of interior faces of the elements with an arbitrarily chosen normal direction n and Γ_{ext} is the set of element faces intersecting with the domain boundary.

The finite element problem then reads: Find $p \in V_k$ such that

$$a(p,v) = l(v) \qquad \forall v \in V_k \tag{16}$$

where the bilinear form is given by

$$a(p,v) = \sum_{E\in\mathcal{T}(\Omega)} \int_E (K\nabla p)\cdot\nabla v \; dV + \sum_{\gamma_e\in\Gamma_{\mathrm{D}}} \int_{\gamma_e} (K\nabla v)\cdot n \; p - (K\nabla p)\cdot n \; v \; ds$$
$$+ \sum_{\gamma_{ef}\in\Gamma_{\mathrm{int}}} \int_{\gamma_{ef}} \langle (K\nabla v)\cdot n\rangle [p] - \langle (K\nabla p)\cdot n\rangle [v] \; ds$$

and the right hand side is the linear form

$$l(v) = \sum_{E\in\mathcal{T}(\Omega)} \int_E f \; v \; dV + \sum_{\gamma_e\in\Gamma_{\mathrm{N}}} \int_{\gamma_e} J \; v \; ds + \sum_{\gamma_e\in\Gamma_{\mathrm{D}}} \int_{\gamma_e} \epsilon\,(K\nabla v)\cdot n \; g \; ds.$$

Here $\langle\cdot\rangle$ denotes the average at the discontinuity and $[\cdot]$ denotes the jump at the discontinuity. This scheme has been introduced in [OBB98].

The problem is discretized on the unit square on the parable shaped subdomain $\Omega^{(0)}$ (see Figure 5).

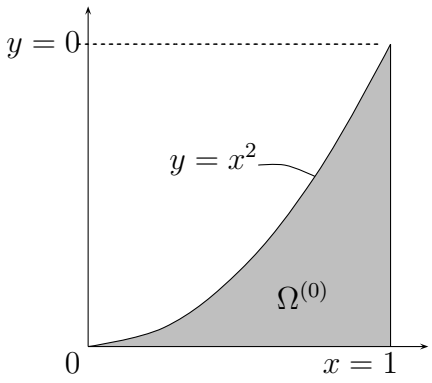

FIGURE 5. Parable shaped subdomain $\Omega^{(0)}$ on the Unit Square.

The test problem has full regularity and will be simulated with two different sets of boundary conditions. First we use only Dirichlet boundary conditions, then we use Neumann boundary conditions on the curved and on the lower boundary and Dirichlet boundary conditions on the right boundary. We choose f, g and J such that the exact solution

$$p(x) = e^{(-||x-x_0||^2)} \qquad \text{with} \qquad x_0 = (0.5, 0.5) \tag{17}$$

is obtained.

Figure 6 shows experimental order of convergence

$$\mathrm{EOC}_k \;=\; \frac{\log(E_{k-1}/E_k)}{\log(2)}. \tag{18}$$

of the L_2- and H^1-error for Dirichlet and Neumann boundary conditions. The calculations are done for trial functions of polynomial degrees 2–5. The graphs on the right side show the

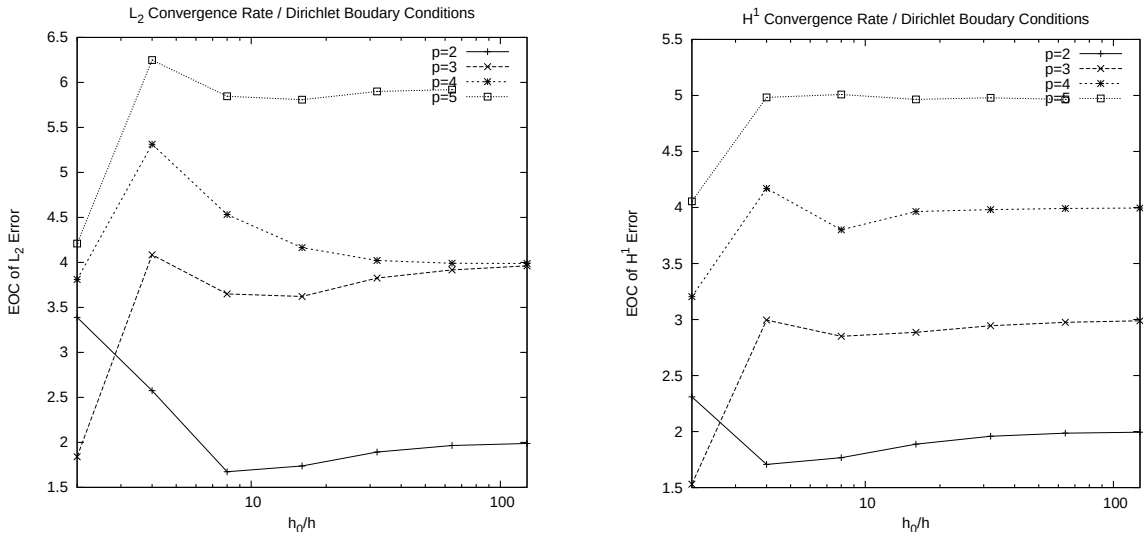

FIGURE 6. Convergence behavior with a cusp element. The plots show the convegence rates for $h \to 0$ for L_2- and H^1-error and dirichlet boundaryconditions. The exact solution is $e^{(-(x-x_0)^2)}$.

Although the cone condition is not fulfilled in this subdomain $\Omega^{(0)}$ (Figure 5) we obtained optimal h-convergence rate in the H^1-norm. The h-convergence in the L_2-norm also exhibits the predicted behavior $O(h^{p+1})$ for p odd and $O(h^p)$ for p even.

5. CONCLUSIONS

We presented a new approach to simulations in complex shaped domains. It is shown experimentally that we obtain optimal convergence rates for the error measured in H^1- and L_2-norm for a scalar elliptic problem.

The scheme is easily applicable for Discontinuous Galerkin discretizations of other partial differential equations.

The disadvantage of the scheme is its high cost for the local triangulation if the grid is very coarse compared with the structure of the partition $\mathcal{G}$.

REFERENCES

[BDGG71] B. L. Buzbee, F. W. Dorr, J. A. George, and G. H. Golub. The Direct Solution of the Discrete Poisson Equation on Irregular Regions. *SIAM Journal on Numerical Analysis*, 8(4):722–736, 1971.

[BH70] J. H. Bramble and S. R. Hilbert. Estimation of Linear Functionals on Sobolev Spaces with Application to Fourier Transformations and Spline Interpolation. *SIAM Journal on Numerical Analysis*, 7(1):112–124, 1970.

[DFS03] V. Dolejsi, M. Feistauer, and V. Sobotikova. Analysis of the Discontinuous GalerkinMethod for Nonlinear Convection–Diffusion Problems. *Preprint*, 2003. Submitted *Comput. Methods Appl. Mech. Eng.*

[EB05] C. Engwer and P. Bastian. A Discontinuous Galerkin method for simulations in complex domains. Technical report, IWR, Univeristy of Heidelberg, 2005.

[GPP71] Rolan Glowinski, Tsorng-Whay Pan, and Kacques Periaux. A fictitious domain method for Dirichlet problem an applications. *Computer Methods in Applied Machanics and Engineering*, 8(4):722–736, 1971.

[HH04] Anita Hansbo and Peter Hansbo. A finite element method for the simulation of strong and weak discontinuities in solid mechanics. *Computer Methods in Applied Mechanics and Engineering*, 193(33-35):3523–3540, 2004.

[HS91] W. Hackbusch and S. A. Sauter. Composite Finite Elements for the Approximation of PDEs on Domains with complicated Micro-Structures. *Preprint*, 1991.

[OBB98] J. T. Oden, I. Babuška, and C. E. Baumann. A discontinuous *hp*-finite element method for diffusion problems. *Journal of Computational Physics*, 146:491–519, 1998.